THE JOURNAL OF PHYSICAL CHEMISTRY B

Article

pubs.acs.org/JPCB

Influences of Mutations on the Electrostatic Binding Free Energies of Chloride Ions in *Escherichia coli* ClC

Tao Yu,[†,⊥] Xiao-Qing Wang,[†,⊥] Jian-Ping Sang,[†] Chun-Xu Pan,[†] Xian-Wu Zou,[†] Tsung-Yu Chen,[‡] and Xiaoqin Zou*[,§]

[†]Department of Physics, Wuhan University, Wuhan 430072, P. R. China

[‡]Center for Neuroscience and Department of Neurology, University of California, Davis, Davis, California 95616, United States

[§]Department of Physics, Department of Biochemistry, Dalton Cardiovascular Research Center, and Informatics Institute, University of Missouri, Columbia, Missouri 65211, United States

ABSTRACT: Mutations in ClC channel proteins may cause serious functional changes and even diseases. The function of ClC proteins mainly manifests as Cl^- transport, which is related to the binding free energies of chloride ions. Therefore, the influence of a mutation on ClC function can be studied by investigating the mutational effect on the binding free energies of chloride ions. The present study provides quantitative and systematic investigations on the influences of residue mutations on the electrostatic binding free energies in *Escherichia coli* ClC (EcClC) proteins, using all-atom molecular dynamics simulations. It was found that the change of the electrostatic binding free energy decreases linearly with the increase of the residue−chloride ion distance for a mutation. This work reveals how changes in the charge of a mutated residue and in the distance between the mutated residue and the binding site govern the variations in the electrostatic binding free energies and therefore influence the transport of chloride ions and conduction in EcClC. This work would facilitate our understanding of the mutational effects on transport of chloride ions and functions of ClC proteins and provide a guideline to estimate which residue mutations will have great influences on ClC functions.

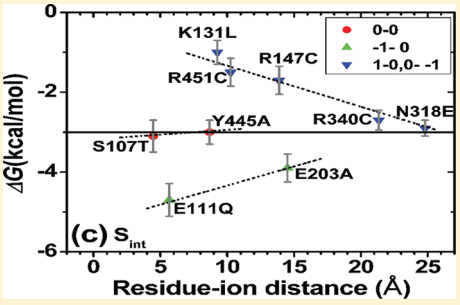

INTRODUCTION

ClC proteins, a large family of membrane proteins that transport chloride ions across cell membranes, play important roles in a variety of physiological processes.[1] Functionally defective ClC mutants in humans cause genetic diseases such as Bartter's syndrome (ClC-Kb), myotonia congenita (ClC-1), Dent's disease (ClC-5), and osteopetrosis (ClC-7).[2−4] It has been reported that mutations in 5 of the 9 human ClC genes lead to genetically inherited diseases.[5]

One of the recent breakthroughs in ClC studies is the three-dimensional crystal structure of the bacterial ClC homologue solved by Dutzler et al. using X-ray diffraction.[6] The structure reveals that ClC is a dimer with two pores. There are three anion binding sites in each pore.[7] The double-barreled structure was previously proposed based on the physiological experiments[8] and is now believed to be common to the entire ClC family. The crystal structure of bacterial ClC provides a platform for investigating the gating and permeation mechanisms of ClC using theoretic methods at the atomic level. Based on the atomic structure, many available theoretic tools have been used to study ClC proteins, such as molecular dynamics,[9−14] Monte Carlo simulation,[15−18] Brownian dynamics,[19] continuous electrostatic calculation method,[4,20,21] and discrete-state model.[20,22]

Interestingly, Accardi and Miller found that the bacterial ClC homologue is a Cl^-/H^+ exchange transporter with stoichiometry 2:1.[23] Afterward, several other ClC proteins were characterized as transporters,[24,25] even though many of the more familiar ClC proteins (such as ClC-0 and ClC-1) still act as passive channels rather than transporters. Many experimental studies on the coupling property of Cl^- and H^+ were performed by Miller and co-workers for the transporter *Escherichia coli* (EcClC).[26−31]

Recently, Lísal and Maduke proposed that some chloride channels are "broken" Cl^-/H^+ transporters,[32] and Mindell suggested that there are deep intertwinings between channel and transporter mechanisms.[33] Indeed, the ClC channels and exchange transporters share many common features.[1,34] Many residues, such as E148, S107, and Y445, are conserved among ClC proteins.

So far, many important residues have been studied both experimentally and theoretically. Regarding ClC channels, the function of a residue is mainly measured by its effect on gating and permeation of channels. From this point of view, the most important residue in EcClC is E148. E148 plays a crucial role on both channels and transporters in the ClC family. This residue occupies a crucial site in the pathway of both Cl^- and H^+ transportations and is a major component of the fast gate. In addition, K131 in EcClC is also an important residue. The side chain of K131 contributes to stabilizing the chloride ions in

Received: January 13, 2012
Revised: May 18, 2012
Published: May 21, 2012

   dx.doi.org/10.1021/jp300430f | *J. Phys. Chem. B* 2012, 116, 6431−6438

the protein.[35] Mutation of R147[36] in EcClC makes the channel nonfunctional. It has also been found that the positively charged R451 and negatively charged E111 are both located near the internal binding site S_{int} and play important roles in channel conduction.[35] Moreover, R340 is found to change the Cl^- permeation.

With respective to ClC transporters, the action of a residue is measured by its effect on proton transport and the coupling of H^+ with Cl^-. In this sense, the most important residues of ClC transporters are E148, Y445, and E203, which are closely associated with the proton pathway and coupling of Cl^- and H^+.[17,34,37] Y445 is situated around the central binding site S_{cen} and directly coordinates a Cl^- ion located near S_{cen}. Thus, Y445 is crucial for the coupled transport of Cl^- and H^+; mutation of Y445 leads to uncoupling.[28,29] Another residue, E203, is located on the intracellular side of the protein and therefore affects only the H^+ transport, not the Cl^- transport. In fact, the mutation of E203 was found to abolish proton transport.[26,37]

Different mutated structures result in different binding free energies. The binding free energy is associated with the height of the energy barrier, which affects the retention time and transport rate of ions in channel proteins. Therefore, the influences of mutations on ClC functions can be studied through investigating the effects of mutations on binding free energies. The first theoretic study on electrostatics of chloride ion stabilization in EcClC was completed in 2004.[4] The work provided insight into future analyses of the permeation and gating processes. However, to our knowledge, no theoretical report has been published on quantitatively studying how mutations change binding free energies. In the present work, we will provide quantitative and systematic investigations on the influences of mutations on electrostatic binding free energies for the chloride ions in EcClC by using all-atom molecular dynamics calculations. The results would be helpful to understand the relationship between mutations and channel conduction. It would also provide insight into estimating which mutations may have important effects on the functions of ClC channels.

METHODS

Construction of the Systems. The structural coordinates of EcClC and a few mutants are available in the Protein Data Bank (PDB). Figure 1 plots EcClC−E148Q. In this figure the chloride ions occupy all the three binding sites: the internal site (S_{int}), central site (S_{cen}), and external site (S_{ext}). To mimic the real situation, EcClC should be placed in the membrane, and the membrane should be immersed in aqueous solution. Specifically, the channel−membrane−water systems were set up as described below.

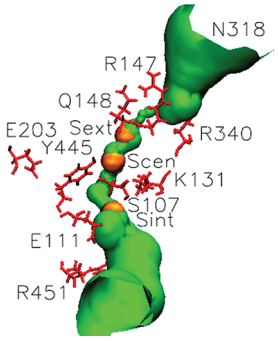

Figure 1. Important residues (shown in red sticks) around the ion-permeation pore (shown in green) in EcClC−E148Q. In EcClC−E148Q there exist three chloride binding sites: S_{ext}, S_{cen}, and S_{int}, referred to as the external, central, and internal site, respectively. The chloride ions at the binding sites are represented by orange van der Waals spheres.

A. Wild-Type EcClC Channel−Membrane−Water System. The wild-type EcClC protein structure was downloaded from the PDB (entry code: 1OTS).[7] The missing hydrogen atoms were added by using PSFGEN of VMD.[38] The residues E113, H175, H281, and H284 of both chain A and chain B and R417 of chain A were protonated[4] using VMD. The N-terminal of each monomer was capped with a neutral acetyl group (ACE), and the C-terminal was capped with an *N*-methyl group (CT3). The binding sites, S_{cen} and S_{int}, were occupied by chloride ions. The constructed channel was then embedded in an explicit POPE membrane with the size of 12 nm × 12 nm. Next, a layer of water with 15 Å of thickness was added to the top and bottom of the membrane, using the VMD software. In addition, 18 Cl^- and 5 Na^+ ions were added in water in order to set the concentration of Cl^- to 100 mM and the total charge of the system to zero. The whole system consisted of 142 999 atoms, in which 13 611 atoms belonged to EcClC, 35 000 to the membrane, and 94 388 to the solution. The atomic charges were assigned with the CHARMM27 force field parameters.[39] The resulted structure is referred to as the initial EcClC−WT channel−membrane−water system, which has not reached equilibrium yet.

To equilibrate the above channel−membrane−water system, the NAMD software[40] was used. First, the initial structure was compacted by running energy minimization for 5000 steps. Then, the refined system was equilibrated by MD simulations under constant NPT condition. In order to minimize the packing voids between the protein−membrane interfaces, NAMD was run for 1 ns by fixing all the protein atoms and Cl^- ions at the binding sites and freeing all the membrane atoms and water molecules. Here, the specified atoms were fixed by using "fixed atoms parameters" in NAMD, namely, by setting the "fixedAtoms" parameter to "on" and by changing the values of the B column in the PDB file from 0.0 to 1.0 for the specified atoms. To equilibrate the whole system, MD simulation was then performed for 16 ns by freeing all the atoms in the system. The temperature was maintained at 300 K, and the pressure was retained at 1 atm. The time step was set to 1 fs. The periodic boundary condition was applied in all the dimensions. Long-range electrostatics was accounted for by using the PME (particle mesh Ewald) algorithm, and the parameters recommended by the NAMD manual were used. The "cutoff distance" and "switching distance" were 12 and 10 Å, respectively. The nonbonded interactions were calculated every 1 time step. The full electrostatic interactions were calculated every 2 time steps. The atoms were reassigned "pair list identities" every 10 time steps. Figure 2a shows the root-mean-square deviation (RMSD) of the backbone atoms of wild-type EcClC as a function of simulation time. It can be seen that the system reached equilibrium after 16 ns.

B. Mutant EcClC Channel−Membrane−Water Systems. To investigate the influences of mutations on electrostatic binding free energies, we considered a series of mutations that are important for channel gating and permeation and constructed the corresponding mutated EcClC channel−membrane−water systems.

dx.doi.org/10.1021/jp300430f | J. Phys. Chem. B 2012, 116, 6431−6438

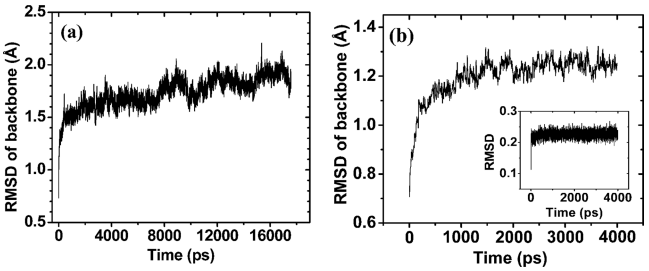

Figure 2. Root-mean-square deviation (RMSD) of the backbone atoms in a trajectory structure as a function of time in the MD simulation. Panel a shows the wild-type EcClC channel−membrane−water system. The initial structure was taken from the experiment crystal structure, followed by energy minimization. The starting time (t = 0) was set to the time when energy minimization was completed, and MD simulation was about to start. Panel b displays the EcClC−E148Q channel−membrane−water system. The starting structure was taken from a partially equilibrated EcClC−E148Q system, in which MD simulation had been performed with the perturbed region by Q148. The inset shows the backbone RMSD when the MD simulation was performed with the atoms in the perturbed region being set to free and the remaining atoms being fixed. See the text for details.

Each initial mutant EcClC channel−membrane−water system was built based on the equilibrated wild-type EcClC channel−membrane−water system, using the program PSFGEN of VMD.[38] However, mutating E148 into glutamine (Q) is an exception. As compared with the experimental structure,[8] the side chain position of Q148 obtained from PSFGEN is downward. Therefore, we manually built the initial EcClC−E148Q channel−membrane−water system by substituting E148 with glutamine in the equilibrated wild-type EcClC channel−membrane−water system, using the position of the side chain of Q148 in the crystal structure of EcClC−E148Q (PDB entry: 1OTU)[7] as a reference. In this initial EcClC−E148Q channel−membrane−water system, all S_{ext}, S_{cen}, and S_{int} sites were occupied.

Next, for each mutated residue, the numbers of Cl^- and Na^+ ions were adjusted to balance the change in the charge of the residue upon mutation. For example, when R451 was mutated to C451, the charge of the residue changed from +1 to 0. Thus, when R451 was replaced by cysteine in the two chains, two Cl^- ions were removed from the electrolyte to preserve the electroneutrality of the system.

It is noticed that the initial mutant system does not deviate much from the equilibrium. Taking the E148Q mutant system as an example, because the initial EcClC−E148Q channel−membrane−water system was established based on the equilibrated wild-type EcClC channel−membrane−water system by converting E148 into glutamine, the mutated residue Q148 affected only its surrounding atoms. Therefore, this mutated system was divided into two regions: the perturbed region and the unperturbed region. The perturbed region consisted of the mutated residue Q148 and all the residues within 12 Å from Q148, which involved a total of 2566 atoms. Because the number of atoms in the perturbed region was small and because the initial structure was not far apart from equilibrium, the equilibration was reached within relatively short simulation time.

The equilibrating process is described as follows. After the energy minimization, the compacted system reached equilibrium through the MD simulation. The MD operation consisted of two steps. The first step was to allow the perturbed region to reach equilibrium. The step was completed by an MD simulation for 4 ns, in which the atoms in the unperturbed region were fixed and the atoms in the perturbed region were set free. The inset of Figure 2b plots the root-mean-square deviation of the backbone atoms in the compacted system. It can be seen from this inset that the perturbed region reached equilibrium after 2 ns. The second step was to equilibrate the whole system, including both the equilibrated perturbed region and the initial unperturbed region, by an MD simulation for 4 ns. Figure 2b plots the root-mean-square deviation of the backbone atoms in the whole EcClC−E148Q system. It can be seen form Figure 2b that the whole system reached equilibrium after 3 ns. Figure 2 shows that the two-step MD simulation method significantly improves the computational efficiency on constructing the mutant EcClC−membrane−water systems.

Calculation of Electrostatic Binding Free Energy. In order to calculate the electrostatic binding free energy, the electrostatic potential and the electrostatic energy of each equilibrated channel−membrane−water system should be calculated. The electrostatic potential Φ is given by the linear Poisson−Boltzmann equation[41,42]

$$-\nabla\cdot(\varepsilon(r)\nabla\Phi(r)) + \bar{\kappa}^2(r)\Phi(r) = 4\pi\sum_{i=1}^{N} q_i\delta(r - r_i) \quad (1)$$

where q_i and r_i are the charge and location of the ith atom, respectively, N is the number of atoms in the system, and $\varepsilon(r)$ denotes the position-dependent dielectric constant. The modified Debye−Hückel parameter $\bar{\kappa} = \varepsilon_w^{1/2}\kappa$ is proportional to the ionic strength of the solution, where κ is the usual Debye−Hückel parameter, and the modification makes $\bar{\kappa}$ dielectric independent. The electrostatic energy of the system is then calculated as

$$\Delta G_{elec} = \frac{1}{2}\sum_{i}^{N} q_i\Phi(r) \quad (2)$$

The above Poisson−Boltzmann equation can be solved numerically by using finite-difference or finite-element methods with a discrete grid, such as APBS,[43] Delphi,[44] ZAP,[45] the PB solver in Amber,[46] and the PBEQ module[47] in CHARMM.[39]

Equation 1 was solved by software APBS 0.5.1, in which a finite element method with a discrete grid was used.[48] The automatically configured sequential method was also applied. The APBS parameters were set as follows. The number of grid points was 161 × 161 × 129. The size of the coarse grid region was 130 Å × 130 Å × 110 Å. The size of the focusing fine grid region was 60 Å × 60 Å × 60 Å, and the size of the fine grid was 0.375 Å × 0.375 Å × 0.469 Å. The whole space was divided into an interior region (explicit structure) and an exterior region (implicit solvent). The explicit structure consisted of the protein and the membrane. The interior region was delimited by the definition of the molecular surface and harmonic average smoothing. The molecular surface was constructed by using a water probe radius of 1.4 Å. Following the CHARMM force field, the radius of the chloride ion was set to 2.27 Å and its charge was set to −1. The dielectric constant ε was set to 4 in the interior region and 78 in the exterior region. The "single Debye−Hückel" boundary condition was used. Following the usual method for charge distribution on grids, the atomic charges in the structure were mapped onto the nearest-neighbor grid points. To minimize discretization effects,

dx.doi.org/10.1021/jp300430f | J. Phys. Chem. B 2012, 116, 6431−6438

translational averaging was implemented in all calculations. The focusing procedure was repeated at eight different locations of the system relative to the center of the 3D grids (shifted by half of a fine grid spacing in each direction), and the results were averaged.

The electrostatic binding free energy $\Delta G_{b,elec}$ of the ith ion is defined as

$$\Delta G_{b,elec} = \Delta G^{is}_{elec} - (\Delta G^{s}_{elec} + \Delta G^{i}_{elec}) \quad (3)$$

where ΔG^{is}_{elec}, ΔG^{s}_{elec}, and ΔG^{s}_{elec} represent the electrostatic energies of the ion-occupied system, the isolated ion-unoccupied system, and the isolated ion in the solvent environment, respectively.

RESULTS AND DISCUSSION

Comparisons of the Electrostatic Binding Free Energies Calculated by Different Methods. To check the feasibility of constructing mutant structures by using the residue substitution method, we made a comparison between the present calculations and the previous calculations. The results are presented in Table 1. The third column of Table 1 lists the results of the previous energy-minimized calculations in which the initial structures were taken from the experimental structures.[4] The fourth column shows the corresponding results of the present study, in which the initial structures were the experimental structure for wild-type EcClC and the modeled structure obtained from the residue substitution method for EcClC−E148Q, respectively. It can be seen that our results are very close to the previous calculations for both wild-type EcClC and EcClC−E148Q. It is noticeable that for EcClC−E148Q our initial structure is different from the experimental structure (PDB entry: 1OTU), which was used for the previous calculations. Despite the different starting structures, the electrostatic binding free energies calculated from the two studies are consistent, indicating the feasibility of constructing mutant structures by using the residue substitution method. Such feasibility is important because most of the mutants of EcClC do not have crystal structures.

Table 1. Comparisons of the Chloride Electrostatic Binding Free Energies Calculated by Different Methods, Including Previous Energy Minimization Calculations,[4] the Present Energy Minimization Calculations, and the Present MD Simulation Calculations[a]

		energy minimization		MD simulation
	binding site	ref 4	present	present
WT	S_{cen}	−9.5(0.3)	−9.1(0.2)	−8.1(0.5)
	S_{int}	−4.4(0.2)	−4.7(0.3)	−2.5(0.3)
E148Q	S_{ext}	−8.8(0.2)	−8.9(0.4)	−8.5(0.4)
	S_{cen}	−10.5(0.2)	−10.3(0.3)	−9.0(0.5)
	S_{int}	−4.6(0.8)	−4.3(0.3)	−3.0(0.4)

[a]The initial structure of wild-type EcClC was taken from the experimental structure in all the three calculations. The initial structure of EcClC−E148Q was taken from the experimental structure (the third column) and built based on the equilibrated wild-type EcClC channel−membrane−water system by substituting E148 with glutamine (the fourth and fifth columns). See text for details about the residue substitution method for the construction of the mutant structures. The energy unit is kcal/mol. The standard deviations are provided in the parentheses.

To compare the differences in the binding free energies obtained before and after the MD simulations, the fifth column of Table 1 lists the electrostatic binding free energies calculated with the structures obtained after the MD simulations, namely, the structures that have reached equilibrium. It can be seen that the results are smaller than the corresponding binding energies calculated with our energy-minimized structures (in the fourth column) for all the three binding sites S_{ext}, S_{cen}, and S_{int}. The differences in the electrostatic binding free energies resulted from the structural changes. In order to show the changes in the protein conformations after the MD simulations, Figure 3 makes a comparison between the initial structure and the equilibrium conformation for wild-type EcClC and the EcClC−E148Q, respectively. Because the energy minimization does not change the atom positions much, the energy-minimized structure is very similar to the initial structure. In contrast, during the MD simulation some atoms may move by large distances. Therefore, it is not surprising that the energy-minimized structure is relatively different from the MD structure and that the absolute values of the electrostatic binding free energies calculated from these two structures are relatively different. Obviously, the binding free energies calculated with MD equilibrated structures are more reliable than the energies calculated with the energy-minimized structures.

Moreover, during an MD simulation the chloride ion at the internal binding site may finally move into the solvent for both wild-type EcClC and EcClC−E148Q. Therefore, the more stable site near the intracellular entrance to the pore was taken

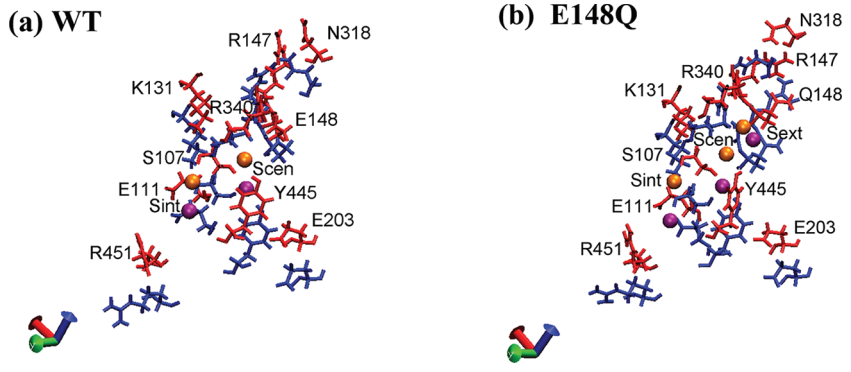

Figure 3. Comparison between the initial structure (red) and the equilibrium structure (blue) for wild-type EcClC (a) and EcClC−E148Q (b). The chloride ions are represented by orange spheres in the initial structure and purple spheres in the equilibrium structure, respectively.

dx.doi.org/10.1021/jp300430f | J. Phys. Chem. B 2012, 116, 6431−6438

Table 2. Chloride Electrostatic Binding Free Energy at the Binding Sites S_{cen} and S_{int} for Wild-Type EcClC and Its Mutants and the Corresponding Mutated Residue−Chloride Ion Distances[a]

	channel	WT	S107T	Y445A	R147C	K131L	E203A	E111Q	R340C	R451C	N318E
S_{cen}											
	energy	−8.1	−7.5	−7.6	−4.8	−5.5	−9.2	−9.8	−6.8	−7.1	−7.2
	distance		4.29	9.08	9.01	12.37	13.35	12.25	14.44	14.89	16.62
S_{int}											
	energy	−2.5	−2.7	−2.4	−1.2	−1.1	−3.1	−3.5	−1.5	−0.7	−2.1
	distance		3.65	8.12	13.72	11.53	15.05	7.87	17.93	9.22	22.37

[a]The unit of energy is kcal/mol. The standard deviations are shown in Figure 4 as error bars. The mutated residue−chloride ion distance is defined as the mean distance between the side chain of a mutated residue and the chloride ion located at a binding site. The unit of length is Å.

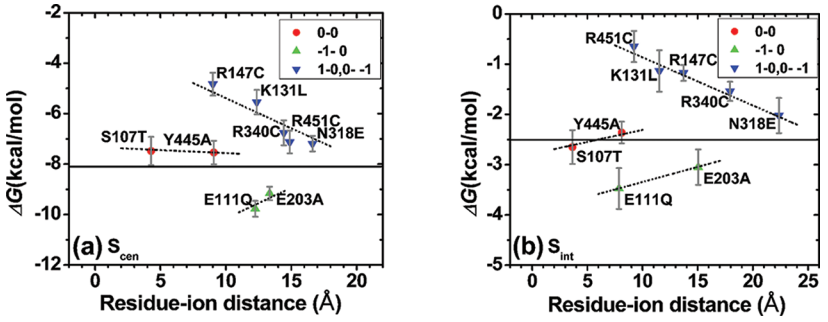

Figure 4. Dependence of the chloride electrostatic binding free energy ΔG on the mutated residue−chloride ion distance for wild-type EcClC. Panel a shows the electrostatic binding free energies at the central site S_{cen}. Panel b shows the energies at the internal site S_{int}. The mutated residue−chloride ion distance is defined as the mean distance between the side chain of the mutated residue and the chloride ion. The symbols show the variation of the residue charge when wild-type EcClC changes into its mutant. The mutations are classified into three categories: The circle symbols stand for mutations that do not change the charges of the residues. The down-triangles represent mutations that reduce individual residue charges by 1. The up-triangles denote mutations that increase individual residue charges by 1. The horizontal lines indicate the electrostatic binding free energies in the wild-type EcClC at individual chloride binding sites. The dotted lines are plotted to help view the variations in ΔG for each category of mutations.

as the internal binding site of the chloride ion in the MD configuration. To explain this procedure, EcClC−E148Q is used as an example. First, we took the internal binding site in the experimental EcClC−E148Q structure as the approximate internal binding site of the equilibrated EcClC−E148Q structure, using the center of the initial EcClC−E148Q configuration as the origin of the coordinate system. Thus, the approximate coordinates of the internal binding site were 15.171 Å, 15.698 Å, and −12.838 Å in the MD configuration of EcClC-E148Q. Here, the coordinates of the binding site were the average values from the MD snapshots. The deviation of each coordinate of the binding sites from the average value was less than 0.5 Å. In order to obtain the accurate position of the internal binding site, a chloride ion was placed at this approximate position, and the system was then equilibrated by the MD simulation. It was found that the chloride ion moved to a new position with the coordinates of 16.397 Å, 12.940 Å, and −15.128 Å and stayed there for a long time (≈2 ns). Therefore, this new position was taken as the internal binding site S_{int} for the MD simulation. At this accurate internal binding site the calculated electrostatic binding free energy was −3.0 kcal/mol, which has an absolute value smaller than the absolute value for the energy-minimized structure (−4.3 kcal/mol), as shown in Table 1. This comparison shows the importance of using a fully equilibrated structure, like the structures obtained from our MD simulations, in chloride binding energy calculations. Therefore, in the rest of the article all the calculations were based on the structures that were equilibrated by MD simulations.

Influences of Mutations on Electrostatic Binding Free Energies. The electrostatic binding free energies were calculated for a series of EcClC mutant channel−membrane−water systems (namely, single mutants) and EcClC−E148Q mutant channel−membrane−water systems (namely, double mutants). The averages were taken over the two protein subunits, and each value of the binding free energy was averaged over at least 10 MD snapshots in the present work. They were randomly chosen from the trajectories with the average value of RMSD to ensure that they were not far apart from equilibrium. The time interval between two adjacent MD trajectories was about 400−500 ps to ensure that the trajectories were independent of each other.

A. For Wild-Type EcClC. For wild-type EcClC there exist only two binding sites, S_{cen} and S_{int}. The electrostatic binding free energy was computed using eq 3. Table 2 lists the electrostatic binding free energies for wild-type EcClC and its mutants.

It is expected that the effect of a mutation on the electrostatic binding free energy depends upon the distance between the residue and the chloride ion and upon the change in the charge of residue before and after the mutation. For simplicity, the residue−chloride ion distance was measured by using the mean distance between the side chain of residue and the chloride ion. A series of residue−chloride ion distances were calculated, as listed in Table 2. Figure 4 plots the dependence of the electrostatic binding free energy on the residue−chloride ion distance for a series of EcClC mutants. To determine the effect of residue charge variations on the electrostatic binding free energy, the changes of residue charges before and after

dx.doi.org/10.1021/jp300430f | J. Phys. Chem. B 2012, 116, 6431−6438

Table 3. Electrostatic Binding Free Energies at the Binding Sites S_{ext}, S_{cen}, and S_{int} for EcClC−E148Q and Its Mutants and the Corresponding Mutated Residue−Chloride Ion Distances[a]

	channel	EcClC−E148Q	S107T	Y445A	K131L	R147C	E111Q	E203A	R340C	R451C	N318E
S_{ext}											
	energy	−8.5	−8.6	−8.6	−6.9	−5.3	−9.8	−10.2	−6.9	−8.1	−6.6
	distance		10.69	14.40	14.22	3.75	17.00	15.37	13.75	21.88	11.37
S_{cen}											
	energy	−9.0	−9.3	−8.8	−7.8	−7.3	−9.8	−10.1	−8.1	−8.4	−8.6
	distance		4.46	8.41	12.50	7.62	11.91	11.79	14.73	15.45	16.65
S_{int}											
	energy	−3.0	−3.1	−3.0	−1.0	−1.7	−4.7	−4.0	−2.7	−1.5	−2.9
	distance		4.47	8.68	9.26	13.89	5.67	14.51	21.34	10.26	24.79

[a]The unit of energy is kcal/mol. The standard deviations are shown in Figure 5 as error bars. The unit of length is Å.

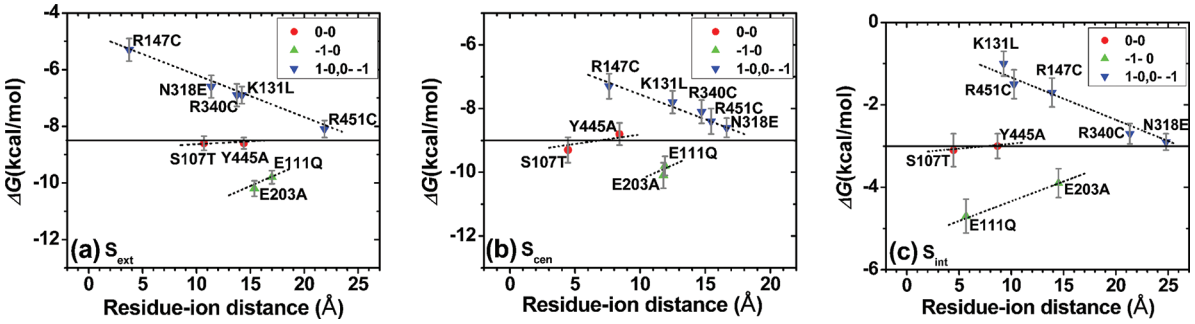

Figure 5. Dependence of the chloride electrostatic binding free energy ΔG on the mutated residue−chloride ion distance for EcClC−E148Q. Panels a−c show the electrostatic binding free energies at the external site S_{ext}, the central site S_{cen}, and the internal site S_{int}, respectively. Other notations are the same as the notations in Figure 4.

mutations are also shown in Figure 4. It can be seen from Figure 4 that if the residue charge becomes more negative after a mutation ($0 \rightarrow -1$ or $1 \rightarrow 0$), the electrostatic binding free energy is less negative (i.e., less favorable) as compared with wild-type EcClC; if the residue charge becomes more positive ($-1 \rightarrow 0$), the electrostatic binding free energy is more negative (i.e., more favorable). The reason is that for an electronegative chloride ion more positive residue makes the attraction increase, and thus the electrostatic binding free energy is more favorable; in contrast, more negative residue increases the repulsion, and therefore the electrostatic binding free energy is less favorable. Accordingly, if the residues remain electroneutrality before and after mutation, the change of the electrostatic binding free energy is minimal upon mutation. Regarding the relationship between the residue−chloride ion distance and the electrostatic binding free energy, Figure 4 also shows that for the same variation of residue charges, the larger the distance, the less the effect of mutations on the electrostatic binding free energy.

It is interesting that there exists a simple and clear law to describe the relationship between the electrostatic binding free energy and the residue−chloride ion distance for such a complex EcClC. It reminds us of the Coulomb's law: The interactive potential energy of two point charges is inversely proportional to the distance between them. In the present investigation the change of the electrostatic binding free energy decreases linearly with the increase of the residue−chloride ion distance when a residue mutation is introduced.

Furthermore, it can be found from Table 2 and Figure 4 that the electrostatic binding free energy and its variation at the internal binding site S_{int} are much less than the corresponding energy and variation at the central binding site S_{cen}. The reason is that the internal binding site is close to the intracellular entrance to the pore and the binding is weak; therefore, the electrostatic binding free energy is small at S_{int}. Consequently, the chloride ion at the internal binding site may move into water with the aid of thermal agitation during the MD simulation. It is conceivable that the effect of mutations on the electrostatic binding free energy at S_{cen} is generally more prominent and important than the effect for S_{int}.

This work reveals how variations in residue charges and residue distances to chloride ions upon mutation govern the changes in electrostatic binding free energies. It therefore provides insight into estimating which mutations may have great influences on the function of EcClC. As mentioned in the Introduction, single mutations such as R147C, K131L, R451C, R340C, and E111Q may damage the Cl^- transport function. Figure 4 explains why: these residues are located near S_{cen} or S_{int}, and their mutations result in change of charges; thus, these mutations lead to prominent changes in the electrostatic binding free energies and affect the transport of chloride ions in EcClC. Previous experiments have also shown that mutations in Y445 and E203 do not impair the Cl^- transport.[24,25,33] This phenomenon results from the facts that Y445A mutation is not accompanied by any change in charges and that the residue E203 is far from the central binding site (see Figure 4). It can be inferred from Figure 4 that the mutations S107T and N318E are not expected to significantly impair the Cl^- transport.

B. For EcClC−E148Q. For channels the action of a residue is mainly measured by its effect on gating and permeation of channels. From this point of view, the most important residue in EcClC is E148. As typical examples of double mutations of wild-type EcClC, mutations and their influences on electrostatic binding free energies for the E148Q mutant were studied.

In EcClC−E148Q there exist three binding sites, S_{ext}, S_{cen}, and S_{int}. The electrostatic binding free energies were computed

dx.doi.org/10.1021/jp300430f | J. Phys. Chem. B 2012, 116, 6431−6438

for EcClC−E148Q and its mutants by using eq 3. The results are listed in Table 3. The residue−ion distance was also calculated for each residue and listed in the table. Figure 5 plots the dependence of the electrostatic binding free energy on the residue−ion distance for EcClC−E148Q.

It can be seen from Figure 5 that for EcClC−E148Q and its mutants the effects of mutations on electrostatic binding free energies are similar to the effects for wild-type EcClC and its mutants: If a residue remains electroneutrality before and after the mutation, the electrostatic binding free energy hardly varies; if the mutation makes the residue charge more negative, the electrostatic binding free energy is less negative (i.e., less favorable); if the mutation makes the residue charge more positive, the electrostatic binding free energy is more negative (i.e., more favorable). In addition, if the mutation does not change the residue charge, the larger the distance, the less the effect on the electrostatic binding free energy.

In general, the residues within 12 Å of distance from the mutated residue would be affected, but in a few cases such as for the mutation Y445A, the distance for influence is larger. Because the side chain of residue Y445 is much larger than that of A445,[29] the mutation Y445A moves the atoms around A445 significantly and the affected region is larger. In this case, 20 Å was taken as the affected distance by Y445A mutation. Our calculations show that for EcClC−E148Q−Y445A when 12 Å was taken as the affected distance, the calculated electrostatic binding free energies caused by Y445A mutation were −8.4, −9.5, and −3.1 kcal/mol at S_{ext}, S_{cen}, and S_{int}, respectively; when 20 Å was used as the affected distance, the corresponding values were −8.6, −8.8, and −3.0 kcal/mol, respectively. It can be seen that for Y445A mutation the two distances (12 Å vs 20 Å) yielded similar calculated electrostatic binding free energies at S_{int} and S_{ext}, but not so for the electrostatic binding free energies at S_{cen}. The reason is because the side chain of Y445 is far from S_{int} and S_{ext}, but close to S_{cen}, so setting 20 Å as the affected distance is important to the calculation of the electrostatic binding free energy at S_{cen} for the Y445A mutation. The similar phenomenon was observed for the Y445A mutation in wild-type EcClC.

CONCLUSION AND DISCUSSIONS

Using all-atom molecular dynamics simulations, we have calculated the electrostatic binding free energies for EcClC and EcClC−E148Q proteins and their mutants and have investigated the influences of mutations on chloride binding free energies.

For the calculations of the electrostatic binding free energies previous studies used the experimental crystal structure of EcClC−E148Q as the initial structure,[4] and we used wild-type EcClC with E148 replaced by glutamine (Q) as the initial structure. Despite different initial structures are used, the calculated electrostatic binding free energies are consistent, which suggests the feasibility of constructing mutant structures by using the residue substitution method. The present study has proposed a useful method to build initial structures for the mutants that lack of crystal structures.

It is found that if the residue charge becomes more negative (or positive) after a residue mutation, the electrostatic binding free energy will be less (or more) favorable. Moreover, the change of the electrostatic binding free energy decreases linearly with the increase of the residue−chloride ion distance when a residue mutation occurs. This work reveals how variation in the charge of the mutated residue and in the distance between the mutated residue and the binding site change the electrostatic binding free energies and thus affect the transport of chloride ions and conduction of EcClC. Our findings provide guidelines to predict which mutations may have great influences on the functions of ClC proteins.

Several lines of investigation remain open for further exploration. First, it is worthwhile to extend the MD simulations from 16 to 50 ns to verify the present results. Second, it is noteworthy to validate the results from the Poisson−Boltzmann equation against a more rigorous free energy calculation over the MD trajectories, such as a thermodynamic integration approach.

AUTHOR INFORMATION

Corresponding Author

*Tel 573-882-6045; Fax 573-884-4232; e-mail zoux@missouri.edu.

Author Contributions

⊥T.Y. and X.-Q.W. contributed equally to this work.

Notes

The authors declare no competing financial interest.

ACKNOWLEDGMENTS

This work was supported by National Institutes of Health (Grant R21GM088517), National Science Foundation Career Award (Grant DBI-0953839), and Postdoctoral Science Foundation of China (Grant 20110491217). Tsung-Yu Chen is partially supported by National Institutes of Health (Grant R01GM065447).

REFERENCES

(1) Chen, T. Y. *Annu. Rev. Physiol.* **2005**, *67*, 809−839.
(2) Iyer, R.; Iverson, T. M.; Accardi, A.; Miller, C. *Nature* **2002**, *419*, 715−718.
(3) Jentsch, T. J.; Stein, V.; Weinreich, F.; Zdebik, A. A. *Physiol. Rev.* **2002**, *82*, 503−568.
(4) Faraldo-Gómez, J. D.; Roux, B. *J. Mol. Biol.* **2004**, *339*, 981−1000.
(5) Jentsch, T. J. *Crit. Rev. Biochem. Mol. Biol.* **2008**, *43*, 3−36.
(6) Dutzler, R.; Campbell, E. B.; Cadene, M.; Chait, B. T.; MacKinnon, R. *Nature* **2002**, *415*, 287−294.
(7) Dutzler, R.; Campbell, E. B.; MacKinnon, R. *Science* **2003**, *300*, 108−112.
(8) Miller, C. *Philos. Trans. R. Soc., B* **1982**, *299*, 401−411.
(9) Moran, O.; Traverso, S.; Elia, L.; Pusch, M. *Biochemistry* **2003**, *42*, 5176−5185.
(10) Cohen, J.; Schulten, K. *Biophys. J.* **2004**, *86*, 836−845.
(11) Bostick, D. L.; Berkowitzy, M. L. *Biophys. J.* **2004**, *87*, 1686−1696.
(12) Bisset, D.; Corry, B.; Chung, S. H. *Biophys. J.* **2005**, *89*, 179−186.
(13) Gervasio, F. L.; Parrinello, M.; Ceccarelli, M.; Klein, M. L. *J. Mol. Biol.* **2006**, *361*, 390−398.
(14) Suenegaa, A.; Yehb, J. Z.; Taijia, M.; Toyamac, A.; Takeuchic, H. *Biophys. Chem.* **2006**, *120*, 36−43.
(15) Miloshevsky, G. V.; Jordan, P. C. *Biophys. J.* **2004**, *86*, 825−835.
(16) Yin, J.; Kuang, Z. F.; Mahankali, U.; Beck, T. L. *Proteins* **2004**, *57*, 414−421.
(17) Kuang, Z. F.; Mahankali, U.; Beck, T. L. *Proteins* **2007**, *68*, 26−33.
(18) Cheng, M. H.; Mamonov, A. B.; Dukes, J. W.; Coalson, R. D. *J. Phys. Chem. B* **2007**, *111*, 5956−5965.
(19) Corry, B.; O'Mara, M.; Chung, S. H. *Biophys. J.* **2004**, *86*, 846−860.
(20) Engh, A. M.; Faraldo-Gómez, J. D.; Maduke, M. *J. Gen. Physiol.* **2007**, *130*, 351−363.

(21) Wang, X. Q.; Yu, T.; Sang, J. P.; Zou, X. W.; Chen, T. Y.; Bolser, D.; Zou, X. *Biophys. J.* **2010**, *99*, 464−471.
(22) Coalson, R. D.; Cheng, M. H. *J. Phys. Chem. B* **2010**, *114*, 1424−1433.
(23) Accardi, A.; Miller, C. *Nature* **2004**, *427*, 803−807.
(24) Picollo, A.; Pusch, M. *Nature* **2005**, *436*, 420−423.
(25) Scheel, O.; Zdebik, A. A.; Lourdel, S.; Jentsch, T. J. *Nature* **2005**, *436*, 424−427.
(26) Accardi, A.; Walden, M.; Ngitragool, W.; Jayaram, H.; Williams, C.; Miller, C. *J. Gen. Physiol.* **2005**, *126*, 563−570.
(27) Nguitragool, W.; Miller, C. *J. Mol. Biol.* **2006**, *362*, 682−690.
(28) Accardi, A.; Lobet, S.; Williams, C.; Miller, C.; Dutzler, R. *J. Mol. Biol.* **2006**, *362*, 691−699.
(29) Walden, M.; Accardi, A.; Wu, F.; Xu, C.; Williams, C.; Miller, C. *J. Gen. Physiol.* **2007**, *129*, 317−329.
(30) Nguitragool, W.; Miller, C. *Proc. Natl. Acad. Sci. U. S. A.* **2007**, *104*, 20659−20665.
(31) Jayaram, H.; Accardi, A.; Wu, F.; Williams, C.; Miller, C. *Proc. Natl. Acad. Sci. U. S. A.* **2008**, *105*, 11194−11199.
(32) Lísal, J.; Maduke, M. *Nat. Struct. Mol. Biol.* **2008**, *15*, 805−810.
(33) Mindell, J. A. *Nat. Struct. Mol. Biol.* **2008**, *15*, 781−783.
(34) Miller, C. *Nature* **2006**, *440*, 484−489.
(35) Chen, M. F.; Chen, T. Y. *J. Gen. Physiol.* **2003**, *122*, 133−145.
(36) Lin, C. W.; Chen, T. Y. *J. Gen. Physiol.* **2000**, *116*, 535−546.
(37) Lim, H. H.; Miller, C. *J. Gen. Physiol.* **2009**, *133*, 131−138.
(38) Humphrey, W.; Dalke, A.; Schulten, K. *J. Mol. Graphics* **1996**, *14*, 33−38.
(39) Mackerell, A. D., Jr.; Bashford, D.; Bellett, M.; Dunbrack, R. L.; Evanseck, J. D., Jr.; Field, M. J.; Fischer, S. *J. Phys. Chem. B* **1998**, *102*, 3586−3616.
(40) Phillips, J. C.; Braun, R.; Wang, W.; Gumbart, J.; Tajkhorshid, E.; Villa, E.; Chipot, C.; Skeel, R. D.; Kale, L.; Schulten, K. *J. Comput. Chem.* **2005**, *26*, 1781−1802.
(41) Gilson, M. K.; Honig, B. *Proteins* **1988**, *4*, 7−18.
(42) Davis, M. E.; McCammon, J. A. *Chem. Rev.* **1990**, *94*, 7684−7692.
(43) Baker, N. A.; Sept, D.; Joseph, S.; Holst, M. J.; McCammon, J. A. *Proc. Natl. Acad. Sci. U. S. A.* **2001**, *98*, 10037−10041.
(44) Rocchia, W.; Alexov, E.; Honig, B. *J. Phys. Chem. B* **2001**, *105*, 6507−6514.
(45) Grant, J. A.; Pickup, B. T.; Nicholls, A. *J. Comput. Chem.* **2001**, *22*, 608−640.
(46) Case, D. A.; Cheatham, T. E.; Darden, T.; Gohlke, H.; Luo, R.; Merz, K. M.; Onufriev, A., Jr.; Simmerling, C.; Wang, B.; Woods, R. *J. Comput. Chem.* **2005**, *26*, 1668−1688.
(47) Jo, S.; Vargyas, M.; Vasko-Szedlar, J.; Roux, B.; Im, W. *Nucleic Acids Res.* **2008**, *36*, 270−275.
(48) Holst, M.; Saied, F. *J. Comput. Chem.* **1993**, *14*, 105−113.